

Characterization of PEO–PAN Hybrid Solid Polymer Electrolytes

N. MUNICHANDRAIAH,¹ G. SIVASANKAR,¹ L. G. SCANLON,² R. A. MARSH²

¹ Department of Inorganic and Physical Chemistry, Indian Institute of Science, Bangalore 560 012, India

² Wright Laboratory/Battery Electrochemistry Section, Wright-Patterson AFB, Ohio 45433–7251

Received 30 June 1996; accepted 31 January 1997

ABSTRACT: Hybrid solid polymer electrolytes (HSPE) of high ionic conductivity were prepared using polyethylene oxide (PEO), polyacrylonitrile (PAN), propylene carbonate (PrC), ethylene carbonate (EC), and LiClO₄. These electrolyte films were dry, free standing, and dimensionally stable. The HSPE films were characterized by constructing symmetrical cells containing nonblocking lithium electrodes as well as blocking stainless steel electrodes. Studies were made on ionic conductivity, electrochemical reaction, interfacial stability, and morphology of the films using alternating current impedance spectroscopy, infrared spectroscopy, and scanning electron microscopy. The properties of HSPE were compared with the films prepared using (i) PEO, PrC, and LiClO₄; and (ii) PAN, PrC, EC, and LiClO₄. The specific conductivity of the HSPE films was marginally less. Nevertheless, the dimensional stability was much superior. The interfacial stability of lithium was similar in the three electrolyte films. © 1997 John Wiley & Sons, Inc. *J Appl Polym Sci* **65**: 2191–2199, 1997

Key words: hybrid solid polymer electrolytes; ionic conductivity; interfacial resistance

INTRODUCTION

In recent years, there has been increasing interest in research and development of rechargeable lithium batteries employing a solid polymer film as an electrolyte.¹ The main advantage anticipated in using a thin film of solid polymer electrolyte (SPE) is essentially to achieve high-energy density of the battery. However, inadequate ionic conductivity of the SPE has been one of the serious problems hampering the progress of this development.

Polyethylene oxide (PEO) has been studied ex-

tensively as a SPE medium following the direction proposed by Wright² and Armand et al.³ Specific conductivity (σ) is of the order of 10^{-8} S cm⁻¹ at ambient temperature, when a SPE film is prepared by complexing PEO with a lithium salt.⁴ Several procedures for preparation of highly conducting ($\sigma \geq 10^{-3}$ S cm⁻¹) SPE films are reported in the literature.^{4–13} These studies include modifications of PEO-based SPE as well as investigations of different polymer media. One of the procedures is to immobilize a solution of propylene carbonate (PrC) and ethylene carbonate (EC) containing a lithium salt (e.g., LiClO₄) in a host polymer.¹³ The immobilization of the solution imparts a high specific conductivity ($\approx 10^{-4}$ S cm⁻¹) to the host polymer, viz., polyacrylonitrile (PAN). The first ever study on PAN electrolyte film was reported by polymerizing acrylonitrile in aqueous solutions containing metal perchlorates.¹⁴ Studies were also reported on preparation of PAN electro-

Correspondence to: N. Munichandraiah.

Contract grant sponsor: U.S. Air Force (European Office of Aerospace Research and Development—UK); contract grant number: C0007.

Journal of Applied Polymer Science, Vol. 65, 2191–2199 (1997)
© 1997 John Wiley & Sons, Inc. CCC 0021-8995/97/112191-09

lyte films using EC, which contained dissolved LiClO_4 .¹⁵ Characterization of the electrolyte film was done in conjunction with lithium metal aiming at a possible application for lithium-based batteries. Also, investigations on lithium cells containing PAN electrolyte films are reported.^{13,16,17} Even though a high specific conductance is achieved with PAN electrolytes, dimensional stability of these films is poor. They are gels rather than solid polymer films. Poor dimensional stability is due to the existence of a liquid solution entrapped in PAN matrix. Unlike PEO, which is a solvent for lithium salts, PAN does not seem to solvate the salts to a significant extent. Indeed, it merely encapsulates the solution in its matrix and the ionic conduction takes place in the liquid medium.

Another approach by adding PrC to a PEO-based solid polymer electrolyte was reported recently.^{18,19} At ambient temperature, specific conductivity (σ) of PEO electrolyte film increased by about three orders of magnitude, owing to the presence of PrC. However, the liquid constituent (viz., PrC) causes the PEO electrolyte film to be wet, thereby affecting its mechanical integrity.

In the present studies, solid polymer electrolyte films consisting of PEO, PAN, PrC, EC, and LiClO_4 were prepared to overcome the above-described problems inherent to PAN and PEO-PrC electrolyte films. The results suggest that these hybrid solid polymer electrolyte (HSPE) films possess good mechanical strength as well as high ionic conductivity. Several characterization studies are reported.

EXPERIMENTAL

Polyethylene oxide (MW: 4×10^6), polyacrylonitrile, and ethylene carbonate were used as received from Aldrich. Propylene carbonate (Aldrich) was distilled under reduced pressure and stored over molecular sieves of grade 4 Å before using. For preparation of HSPE films, appropriate quantities of PEO, PrC, EC, and LiClO_4 were first dissolved in acetonitrile. After adding the required quantity of PAN, the solution was stirred for several hours. A homogeneous suspension was obtained. A film was cast by spreading the suspension on Teflon-covered glass plates and allowing acetonitrile to evaporate slowly. Finally, the film was dried at 80°C under vacuum for about 10 h. The resulting HSPE film was visually examined for its dry and free-standing nature.

For the purpose of comparison, (i) films con-

sisting of PEO, PrC, and LiClO_4 , and (ii) gel films of PAN, PrC, EC, and LiClO_4 were also prepared. While the former SPE film was prepared by solution casting technique, the gel film was prepared by mixing the required quantities of the constituents thoroughly and heating the mixture in a glass petridish at 90°C for about 5 min. On cooling, a transparent gel film was obtained.

Symmetrical cells of the type: SS/SPE/SS and (SS)Li/SPE/Li(SS) were assembled in an argon-filled dry box. SS refers to a stainless steel disc with an integral lead. The SS disc was in contact with SPE as a blocking electrode in the former type of cells. It was contacting Li electrode in the latter type of cells. The nonblocking Li electrode of 1 cm² area was punched from 0.75 mm thick Li ribbon supplied by Aldrich. The cells were assembled in Teflon holders and were contained in airtight glass containers that had provision for taking electrical contacts. The glass container of the cell was heated to a defined temperature by using a heating tape and a temperature controller. The cell was kept to equilibrate at the set temperature, maintained within $\pm 1^\circ\text{C}$, for about 2 h prior to the experiment. Experiments were carried out at different temperatures between ambient temperature and 100°C.

Electrochemical impedance spectroscopic studies of the symmetrical cells were performed in the frequency range between 100 mHz and 100 kHz using Electrochemical Impedance Analyzer PARC (EC&G) Model 6310. The analysis of the data was carried out using the computer program written by Boukamp and supplied by PARC (EG&G). Cyclic voltammograms of the cells were recorded by using Polarographic Analyzer PARC (EG&G) Model 174A and Omnigraph recorder. Samples of SPE films were examined under Cambridge Instruments Scanning Electron Microscope model S-360. Very thin films (5–10 μm thick) of HSPE films were sandwiched between KBr windows, and IR spectra were recorded using Nicolet FTIR Spectrometer model Impact 400D driven by Omnic software.

RESULTS AND DISCUSSION

The aim of the present investigations was to prepare dry and dimensionally stable HSPE films and to characterize them for ionic conductivity as well as the electrochemical reaction occurring at the Li/HSPE interface. While the blocking SS/HSPE/SS cells were used for conductivity measurements, the nonblocking (SS)Li/HSPE/

Li(SS) were employed for studies related to the electrochemical reaction.

Electrochemical Impedance Spectroscopy

The impedance spectrum of (SS)Li/HSPE/Li(SS) recorded at ambient temperature is shown in Figure 1 as Nyquist and Bode plots.²⁰ Spectra recorded at higher temperatures also resembled Figure 1 in shape. As perceived from the data of Figure 1, the electrical equivalent circuit of the symmetrical cell in the frequency domain of present studies is shown in Figure 2. Resistance of the polymer film is represented by R_b , resistance associated with the charge-transfer reaction at the Li/HSPE interface by R_i , and the corresponding interfacial capacitance by C_i . Behavior of the parallel combination of R_i and C_i is represented by a characteristic semicircle dispersion of the real (Z') and imaginary ($-Z''$) components of the impedance spectrum [Fig. 1(a)], as expected. The polymer electrolyte film usually exhibits the behavior of a capacitance (C_g), which is considered parallel to R_b (not shown in Fig. 2). A high-frequency semicircle expected for parallel R_b and C_g was not obtained [Fig. 1(a)], due to the fact that the R_b of the polymer electrolyte film was low and the maximum frequency was limited to 100 kHz, which was a limitation of the equipment. The high-frequency intercept of Figure 1(a) provided the ionic resistance (R_b) of the electrolyte film. The diameter or the low-frequency intercept of the semicircle provided the interfacial resistance (R_i).

The specific conductivity (σ) at the SPE was calculated using the following equation:

$$\sigma = l/R_b A \quad (1)$$

where l is the thickness of the electrolyte film and A its cross-sectional area (= area of the electrode).

The interfacial resistance (R_i) represents the kinetics of the electrochemical reaction between Li metal and Li^+ ion in the solid polymer electrolyte film:



The exchange current density (I_o) of reaction (2) was evaluated as

$$I_o = RT/FAR_i \quad (3)$$

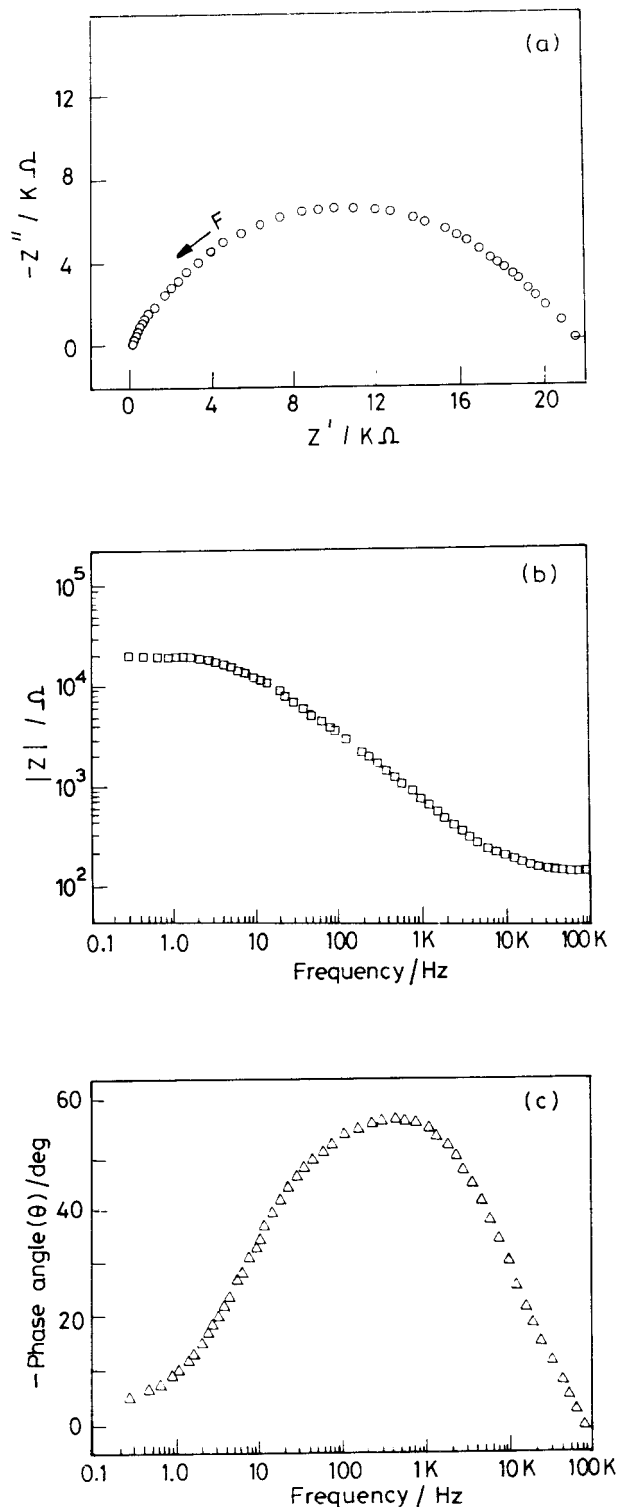


Figure 1 Electrochemical impedance spectrum of (SS)Li/HSPE/Li(SS) cell shown as (a) Nyquist plot, (b) Bode-impedance (Z) plot, and (c) Bode-phase angle (θ) plot. Temperature = 25°C, thickness of HSPE = 250 μm , cross-sectional area = 1.0 cm^2 .

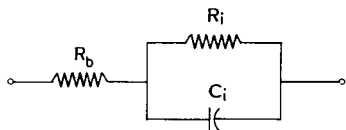


Figure 2 Electrical equivalent circuit of (SS)Li/HSPE/Li(SS) cell, R_b is the resistance of the polymer electrolyte film; R_i and C_i are interfacial resistance and capacitance, respectively.

Although eq. (3) is generally applied to a reaction occurring at a film-free metal, it is also used frequently to evaluate reaction (2) occurring at Li metal, which is covered with an inherent passive film.²¹ Reaction (2) proceeds through the passive film present between the Li metal and the electrolyte film. Interfacial resistance (R_i) may, therefore, be considered to have contributions from reaction (2) as well as the passive film. The existence of the passive film with its resistance and capacitance in parallel, however, was not observed in the form of an additional high frequency semicircle in Figure 1(a). Hence, contribution of passive film to R_i was neglected and I_o was calculated using eq.(3).

In the Bode form of the impedance plots [Fig. 1(b)], capacitance behavior of the symmetrical cell is reflected in a linear decrease of $\log Z$ in middle frequency domain, where Z is modulus of impedance. The constancy of Z at low- and high-frequency domains suggests resistive behavior of the cell. Accordingly, the phase angle (Θ) approaches -60° in the middle frequency domain, which is close to -90° theoretically expected for capacitive behavior. In low- and high-frequency domains Θ approaches zero [Fig. 1(c)].

The impedance spectrum of a SS/SPE/SS cell is shown in Figure 3. The Nyquist plot [Fig. 3(a)] contains all data points on a straight line instead of a semicircle. There is a decrease in $\log Z$ with frequency up to about 1 kHz following, where it remains constant [Fig. 3(b)]. The phase angle Θ is about -75° at the low-frequency domain [Fig. 3(c)], suggesting capacitive behavior of the cell. There is a shift in the value of Θ towards zero with an increase of frequency, which means that the impedance of the cell is dominated by a resistor in the high-frequency domain. These results suggest a series combination of a resistor and a capacitor. The equivalent circuit of SS/HSPE/SS cell thus is as shown in Figure 4. The resistance (R_b) of the HSPE film is in series with the double-layer capacitance (C_{dl}) at the stainless steel elec-

trode/HSPE interface. The intercept of the straight line in Figure 3(a) was taken as R_b and σ was calculated using eq. (1). It was found that

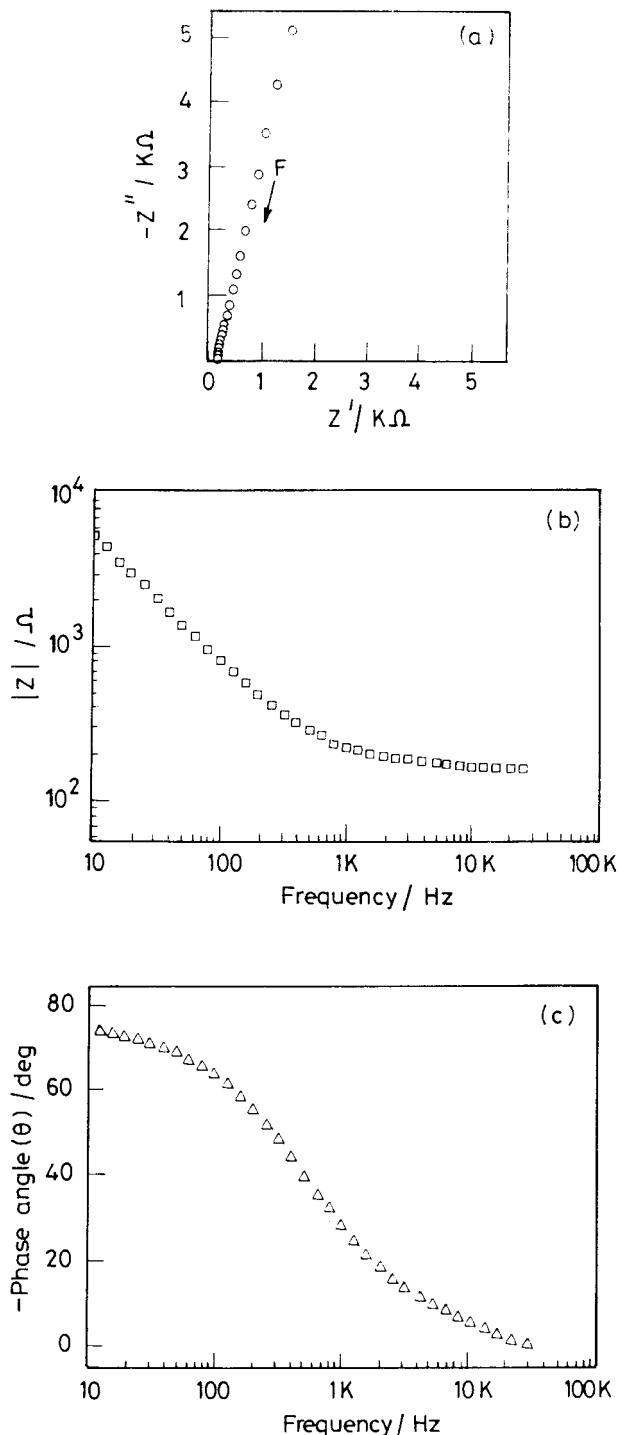


Figure 3 Electrochemical impedance spectrum of SS/HSPE/SS cell shown as (a) Nyquist plot, (b) Bode-impedance (Z) plot, and (c) Bode-phase angle (Θ) plot. Temperature = 30°C , thickness of HSPE = $250\ \mu\text{m}$, cross-sectional area = $0.5\ \text{cm}^2$.

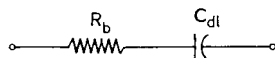


Figure 4 Electrical equivalent circuit of SS/HSPE/SS cell. R_b is the ionic resistance of the polymer electrolyte film, and C_{dl} is the double-layer capacitance.

the value of σ of a given SPE was invariant when measured using either SS/SPE/SS or (SS)Li/SPE/Li(SS) cells. The values of R_b and R_i were found reproducible within $\pm 5\%$ error. Accordingly, the same error is involved in the values of σ and I_o .

Ionic Conductivity

It was intended to arrive at an appropriate composition of HSPE on the basis of high specific conductivity achievable with HSPE film when it was dry with good dimensional stability. The HSPE consists of several components, viz., PEO, PAN, PrC, EC, and LiClO_4 , and, therefore, experiments required for arriving at an appropriate composition, taking into account all components and their contributions, are rather large in number. As the enhancement in conductivity was considered due to the presence of PrC and EC, several HSPE films were prepared only by varying the concentration of PrC and EC while maintaining concentrations of other components nearly invariant. The conductivity (σ) of the HSPE films is shown at different temperatures in Figure 5 as a function of $[(\text{PrC}+\text{EC})/\text{LiClO}_4]$ mol ratio. It is evident that the HSPE film having 3.67 mol ratio of $[(\text{PrC}+\text{EC})/\text{LiClO}_4]$ exhibits the highest conductivity at all temperatures. The composition of this film with $\sigma = 0.37 \text{ mS cm}^{-1}$ at 30°C is shown in Table I, together with the composition of PEO+PrC and PAN+PrC+EC electrolyte films. The conductivity ($\sigma = 0.37 \text{ mS cm}^{-1}$) of the HSPE film is slightly less than $\sigma (=0.84 \text{ mS cm}^{-1})$ of PEO+PrC and $\sigma (=1.34 \text{ mS cm}^{-1})$ of PAN+PrC+EC films. The advantage, however, is that the HSPE film is dry with good mechanical stability.

It is clear from the composition of the HSPE as well as from IR spectrum (cf. Infrared Spectroscopy section) that ionic conduction should, in principle, occur parallelly on two different paths viz., segmental motion of PEO chains and ionic mobility in the liquid medium (PrC and EC). The relative contribution of these two paths, however, is not reflected in the impedance diagrams. It is probably due to the fact that there is a wide differ-

ence in σ of the two paths. The value of σ is about $10^{-8} \text{ S cm}^{-1}$ in PEO- LiClO_4 medium, whereas it is about $10^{-3} \text{ S cm}^{-1}$ or higher in PC-EC- LiClO_4 medium at ambient temperature.

The temperature dependence of σ of the three films given in Table I is shown in Figure 6. The results are found to follow the Arrhenius relation. The energies of activation of conduction for films numbered I, II, and III in Table I are 33.8, 25.2, and 25.9 kJ mol^{-1} , respectively. Similar values of activation energy are reported for PAN-based electrolytes.¹⁷

Electrochemical Reaction

The values of exchange current density (I_o) of reaction (2) at 30°C in the three electrolytes are given in Table I. The value of I_o is slightly lower in HSPE than in PEO+PrC and PAN+PrC+EC electrolyte films. Exchange current values about three orders of magnitude higher than the present values were reported for reaction (2) in similar highly conducting polymer or gelled electrolyte films.²² These studies, however, were made with freshly deposited lithium on a nickel substrate. The lower values of I_o obtained in the present studies can be attributed to a native surface passive film present on Li used for making the cells. The cyclic voltammograms recorded at scan rates ranging from $10\text{--}200 \text{ mV s}^{-1}$ did not contain current peaks in both cathodic and anodic potential sweeps. Instead, a steady-state type of voltammograms with limiting currents were obtained. This suggests that the electron-transfer rate is slower than the rate of diffusion of Li^+ ions at Li/SPE interface. These observations prevailed in the three types of electrolyte films. The reason for not obtaining current peaks is probably due to highly resistive passive film that was already formed on Li before recording voltammograms. The cells were sufficiently aged and subjected to high temperature measurements prior to recording voltammograms. These factors are responsible for the presence of resistive and thicker passive layer on Li.

Influence of Aging of the Cells

The complex plane impedance plots at different intervals of ambient temperature aging of a (SS)Li/HSPE/Li(SS) cell are shown in Figure 7. It is seen that both the high- and low-frequency intercepts on real axis keep shifting towards higher values. Specific conductivity (σ) and interfacial resistance (R_i) are shown as a function

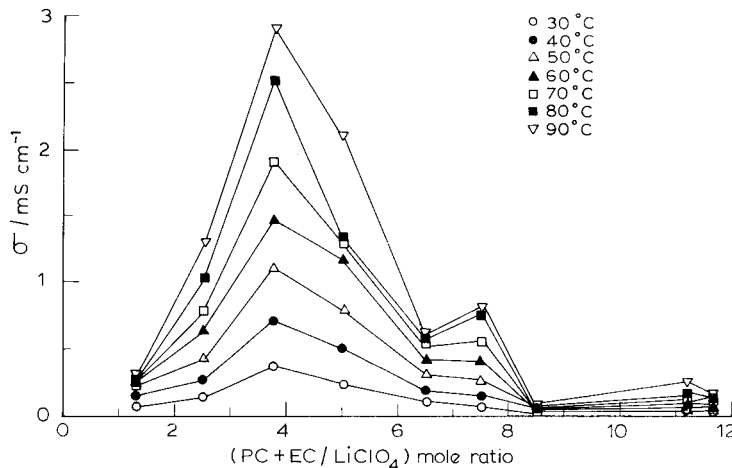


Figure 5 Specific conductivity (σ) as a function of (PrC+EC/LiClO₄) mol ratio at different temperatures.

of aging time in Figures 8 and 9, respectively. It is seen that σ decreases, whereas R_i increases. When Li metal is in contact with the solid polymer electrolyte film, it tends to undergo oxidation (or corrosion) and the reaction products accumulate resulting in the formation of a passive film on Li. As the aging time progresses, the passive film grows in thickness. Because the reaction (2) has to proceed through the passive film, it experiences a higher resistance (R_i) with increasing aging time. Accordingly, exchange current density of the reaction decreases.

The decrease in σ (Fig. 8) is also attributed

to the corrosion of Li metal. The three types of electrolyte films contain liquid components viz., PrC and EC. It is known that Li is thermodynamically unstable when in contact with PrC or EC electrolytes. The liquid solvent molecules undergo reductive decomposition, which in turn, facilitates the oxidation of Li metal. The decrease in σ on aging may be due to loss of PrC and EC molecules in the electrolyte film. This process leads to changes in composition of the electrolyte film with respect to liquid phase and overall Li⁺ ion concentration in the composite medium. The concentration of Li⁺ ions can also be considered to change

Table I Composition of Polymer Electrolyte Films with Specific Conductivity (σ) and Exchange Current Density (I_o) of Lithium Electrode Reaction at 30°C

Film	Composition			σ mS cm ⁻¹	I_o μ A cm ⁻²
	Component	in mM	in Gram		
(I) HSPE	PEO	22.7	1.000	0.37	1.3
	PAN	17.4	0.750		
	PrC	7.3	0.750		
	EC	8.5	0.750		
	LiClO ₄	4.3	0.450		
(II) PEO + PrC	PEO	22.7	1.000	0.84	11.0
	PrC	13.3	1.366		
	LiClO ₄	1.2	0.123		
(III) PAN + PrC + EC	PAN	23.2	1.000	1.34	3.7
	PrC	24.5	2.500		
	EC	28.4	2.500		
	LiClO ₄	3.0	0.320		

mM of PEO and PAN are calculated based on the molecular weight of a repeat unit of the polymer.

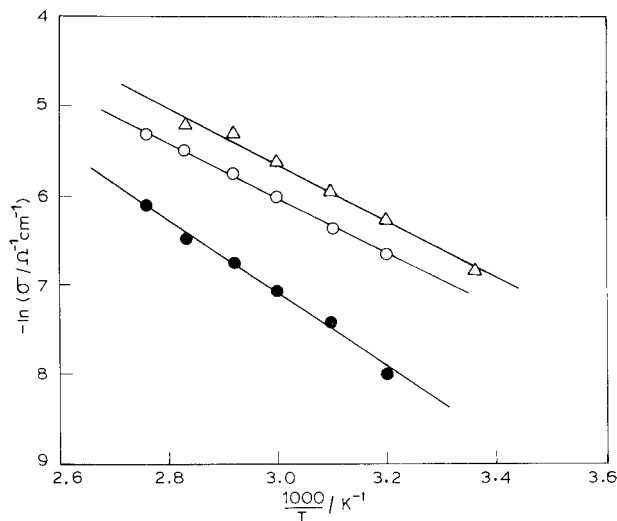


Figure 6 Arrhenius plots of specific conductivity (σ) of HSPE (●), PEO+PrC (○), and PAN+PrC+EC (Δ) electrolyte films.

due to partial and slow dissolution of outer layers of passive film into the electrolyte medium. Cells containing the three types of electrolyte films show similar behavior on aging. During the course of aging, the cells were occasionally heated to several temperatures up to 100°C for the purpose of impedance and cyclic voltammetric measurements. All cells, however, were not uniformly subjected to heating and cycling. Because heating and cycling of the cells influence the passive film on Li, and passive film, in turn, influences σ and R_i ,

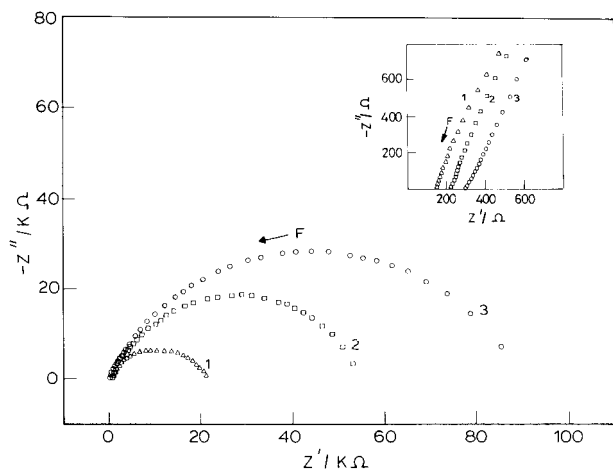


Figure 7 Nyquist plots of (SS)Li/HSPE/Li(SS) cell measured at 48 h (1), 144 h (2), and 312 h (3) after the cell was assembled and aged at ambient temperature. The high-frequency intercept is expanded and shown in the inset.

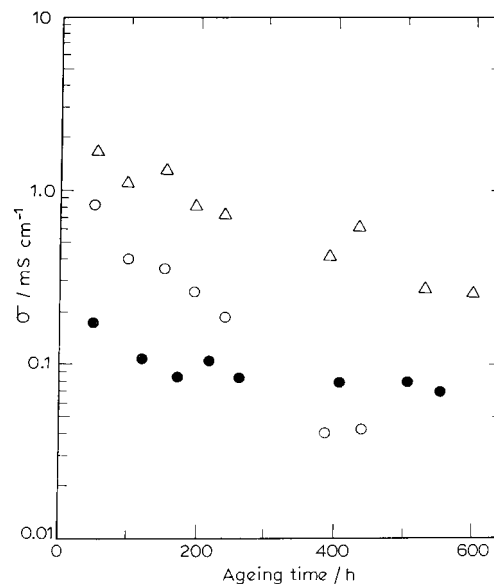


Figure 8 Specific conductivity (σ) of HSPE (●), PEO+PrC (○), and PAN+PrC+EC (Δ) electrolyte films as a function of aging time at ambient temperature.

the results shown in Figures 8 and 9 are only qualitative in nature.

Infrared Spectroscopy

The FTIR spectrum of a thin film of HSPE is shown in Figure 10. The peaks were assigned

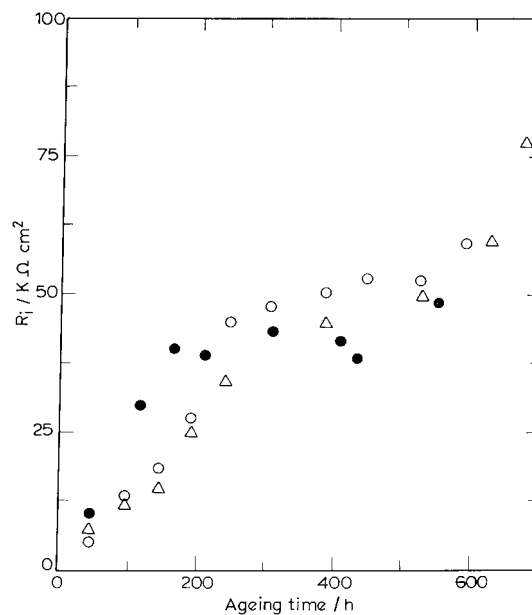


Figure 9 Interfacial resistance (R_i) at the interface between Li and HSPE (●), PEO+PrC (○), and PAN+PrC+EC (Δ) electrolyte films as a function of aging time at ambient temperature.

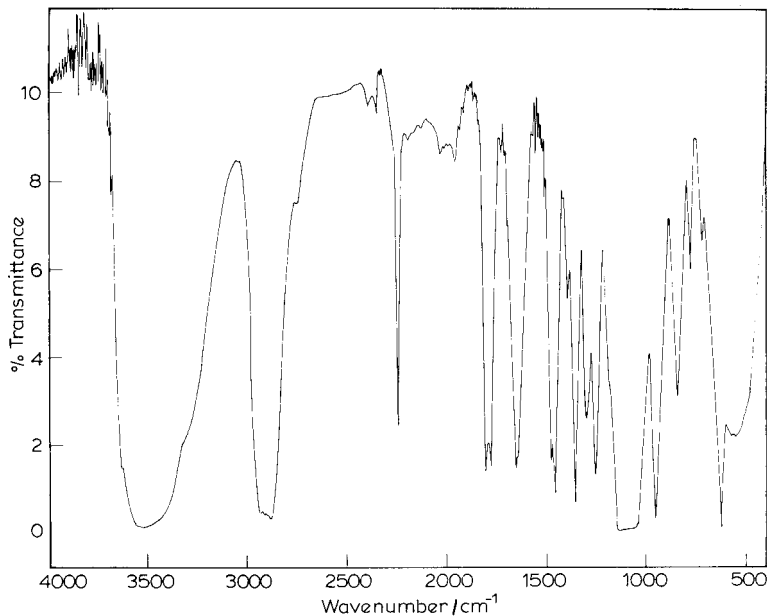


Figure 10 FTIR spectrum of a thin film of HSPE.

by comparing this spectrum with the spectra of individual components of the HSPE, which are reported in the literature.^{23–25} The peak at wave number 958 cm^{-1} can be assigned to $\text{Li}^+ - \text{PrC} - \text{ClO}_4$ interaction.²³ A broad band in the range of wave number 1050 cm^{-1} to 1150 cm^{-1} appears to be a characteristic feature of PEO when combined with alkali metal salts or other materials.²³ It is thus inferred that coordination between Li^+ ion and etherial oxygen of PEO chain exists, suggesting that LiClO_4 is soluble in PEO as well as in PrC and EC. Although Li^+ ions are present in different chemical environments within HSPE, they are not distinguishable by impedance data, as discussed in the Ionic Conductivity section.

Scanning Electron Microscopy

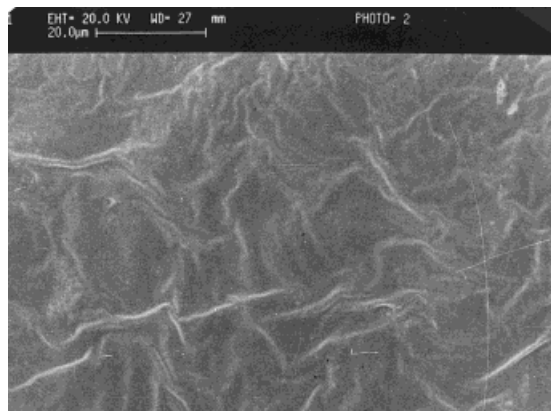
SEM micrographs of $\text{PEO} + \text{LiClO}_4$ and $\text{PEO} + \text{PAN} + \text{PrC} + \text{EC} + \text{LiClO}_4$ films are shown in Figure 11. From the micrographs of $\text{PEO} + \text{LiClO}_4$ [Fig. 11(a)], it is inferred that the electrolyte is homogeneous. In Figure 11(b), long interlocked chains of PAN are clearly found. The liquid components viz., PrC and EC containing LiClO_4 together with PEO, are probably encapsulated within the interlocked network. This type of structure is perhaps responsi-

ble for retaining the liquid components within the film and keeping the surface of the film dry.

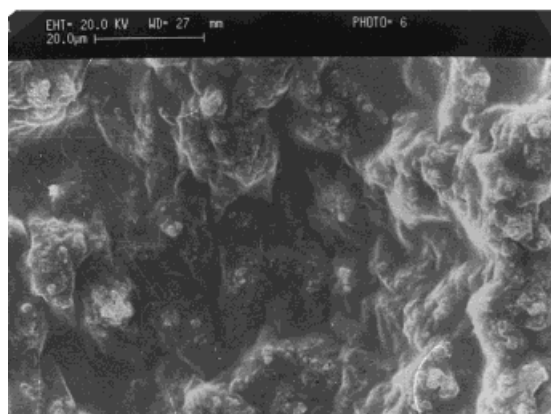
CONCLUSIONS

The hybrid polymer electrolyte films studied in the present investigations exhibit ionic conductivities in the range of 10^{-4} S cm^{-1} at ambient temperature. This value is much higher than the conductivity of conventional PEO-based polymer electrolyte films ($\sigma \approx 10^{-8}\text{ S cm}^{-1}$). Even though there is a marginal decrease in σ in comparison with $\text{PEO} + \text{PrC}$ and $\text{PAN} + \text{PrC} + \text{EC}$ electrolyte, the advantage achieved with HSPE film is that it is dry and free standing with dimensional stability as good as the PEO polymer electrolyte film. The present studies further provide implication on the aging effect of Li in $\text{PEO} + \text{PrC}$ and $\text{PAN} + \text{PrC} + \text{EC}$ electrolyte, which are investigated as highly conducting SPE films. Although these electrolyte films and also HSPE films described in the present work perform with high ionic conductivity in freshly prepared solutions, the conductivity gradually decreases on aging.

Although an attempt is made in the present work to arrive at an appropriate composition of a dry, free-standing, and dimensionally stable HSPE with high specific conductivity, there is still scope for further studies in this direction. As the HSPE contains several constituents, an appro-



(a)



(b)

Figure 11 Scanning electron micrograph of (a) PEO+LiClO₄ film and (b) HSPE film.

appropriate method is based on statistical optimization of the composition. Studies in this direction are being taken up in our laboratory.

Financial support of this work by U.S. Air Force through their European Office of Aerospace Research and Development (UK) under Contract No. C0007 is gratefully acknowledged. The authors thank Dr. M. Durga Prasad and Dr. T.S. Balasubramanian of Renewable Energy Systems Ltd., Hyderabad (India) for providing cell-fabrication facilities, Dr. P.V. Kamath for FTIR spectra, and Mr. Sam Philip for SEM micrographs.

REFERENCES

1. M. Gauthier, A. Bilanger, B. Kapfer, G. Vassort, and M. Armand, in *Polymer Electrolyte Reviews—*
2. J. R. MacCallum and C. A. Vincent, Eds., Elsevier Applied Science, London, 1989.
3. P. V. Wright, *Br. Polym. J.*, **7**, 319 (1975).
4. M. B. Armand, J. M. Chabagno, and M. J. Duclot, in *Fast Ion Transport in Solids*, P. Vashista, J. N. Mundy, and J. K. Shenoy, Eds., North-Holland, Amsterdam, 1979, p. 131.
5. N. Munichandraiah, L. G. Scanlon, R. A. Marsh, B. Kumar, and A. K. Sircar, *J. Appl. Electrochem.*, **25**, 857 (1995).
6. N. Munichandraiah, L. G. Scanlon, R. A. Marsh, B. Kumar, and A. K. Sircar, *J. Appl. Electrochem.*, **24**, 1066 (1994).
7. B. Kumar and L. G. Scanlon, *J. Power Sources*, **52**, 261 (1995).
8. J. Przyluski, K. Such, H. Wycislik, W. Wiczorek, and Z. Florianczyk, *Synth. Met.*, **35**, 241 (1990).
9. J. Plochanski and W. Wiczorek, *Solid State Ionics*, **28**, 979 (1988).
10. G. Nagasubramanian, A. I. Attia, G. Halpert, and E. Peled, *Solid State Ionics*, **67**, 51 (1993).
11. R. Hug, G. C. Farrington, R. Koksang, and P. E. Tonder, *Solid State Ionics*, **57**, 277 (1992).
12. M. L. Kaplan, E. A. Reitman, and R. J. Cava, *Polymer*, **30**, 504 (1989).
13. R. Xue, H. Huang, X. Huang, and L. Chen, *Solid State Ionics*, **74**, 133 (1994).
14. K. M. Abraham and M. Alamgir, *J. Electrochem. Soc.*, **137**, 1657 (1990).
15. S. Reich and I. Michaeli, *J. Polym. Sci.*, **13**, 9 (1975).
16. M. Watanabe, M. Kanba, and K. Nagaoka, *J. Polym. Sci.*, **21**, 939 (1983).
17. G. Feuillade and Ph. Perche, *J. Appl. Electrochem.*, **5**, 63 (1975).
18. H. Hong, C. Lique, H. Xuejie, and X. Rongjian, *Electrochim. Acta*, **37**, 1671 (1992).
19. M. Z. A. Munshi and B. B. Owens, *Solid State Ionics*, **26**, 41 (1988).
20. R. Xue, H. Huang, X. Huang, and L. Chen, *Solid State Ionics*, **74**, 133 (1994).
21. P. G. Bruce, in *Polymer Electrolyte Reviews—I*, J. R. MacCallum and C. A. Vincent, Eds., Elsevier Applied Science, London, 1987.
22. E. Peled, in *Lithium Batteries*, J. P. Gabano, Ed., Academic Press, London, 1983, p. 43.
23. A. M. Christie and C. A. Vincent, *J. Appl. Electrochem.*, **26**, 255 (1996).
24. B. L. Papke, M. A. Ratner, and D. F. Shriver, *J. Phys. Chem. Solids*, **42**, 493 (1981).
25. D. Battisti, G. A. Nazri, B. Klassen, and R. Arora, *J. Phys. Chem.*, **97**, 5826 (1993).
26. P. Bajaj, K. Sen, and S. Hajirahmani, *J. Appl. Polym. Sci.*, **59**, 1539 (1996).